Proton Nuclear Magnetic Resonance Spectroscopy and Ligand Binding Dynamics of the *Escherichia coli* L-Arabinose Binding Protein†

Abbot F. Clark,‡ Thomas A. Gerken, and Robert W. Hogg*

ABSTRACT: The L-arabinose binding protein (ABP) from *Escherichia coli* was studied by proton nuclear magnetic resonance spectroscopy (^{1}H NMR). Distinct spectral changes occur when ABP binds its natural ligand, L-arabinose, which involve resonances in the aromatic ring current shifted methyl, bulk methyl, methylene, aromatic, and amide proton regions of the spectra. Several amide resonances can be "protected" from deuterium exchange if L-arabinose is bound to ABP prior to deuterium oxide dialysis. On the basis of the pH dependence of their chemical shifts, two low-field resonances have been tentatively assigned to C2 protons of two of the three histidines present in ABP. These histidyl residues have pK values of 8.0 and 8.6 which support their involvement in ionic interactions observed earlier in the crystallographic analysis. One histidyl residue shows a small chemical shift change upon the addition of arabinose. When ABP binds D-galactose, changes in the spectra occur which are different than those observed when L-arabinose is bound. Binding of L-arabinose and D-galactose to the binding protein (ABP) was considered by equilibrium binding and fluorescence emission spectroscopy. ABP binds L-arabinose and D-galactose with high affinities (K_d's at 6 °C of 1.3×10^{-7} and 1.9×10^{-7} M, respectively), and both enthalpy and entropy contribute to the ABP–ligand association. When excited at 285 nm, ABP has a fluorescence emission maximum of 340 nm which is quenched and blue shifted (to 337 nm) upon binding L-arabinose. ABP binding D-galactose produced a similar emission shift but no fluorescence quenching.

Gram-negative enteric bacteria contain a number of periplasmic binding proteins which are essential for the high-affinity transport of many sugars, amino acids, and ions (Boos, 1974). Several of these molecules also serve as receptors during bacterial chemotaxis (Alder, 1975; Koshland, 1977). Binding proteins are released from the periplasm by osmotic shock treatment (Neu & Heppel, 1965) with concomitant loss of transport activity and have a high affinity (K_d's of 10^{-6}–10^{-8} M) and specificity for ligand binding.

Upon binding ligand, such periplasmic binding proteins must signal specific integral membrane proteins that they are ready to participate in these designated processes. In several cases, conformational changes have been reported when periplasmic binding proteins bind their respective ligand (Boos & Gordon, 1971; Boos, 1972; Langridge et al., 1970; Weiner & Heppel, 1971; McGowan et al., 1974; Szmeleman et al., 1976; Kreishman et al., 1973; Robertson et al., 1977; Manuck & Ho, 1979; Parsons & Hogg, 1974; Quiocho et al., 1980); however, the techniques used often did not differentiate between local changes around the residues involved in ligand binding from global changes in protein conformations.

The L-arabinose binding protein (ABP)[1] is the first periplasmic binding protein to have an established primary and tertiary structure (Hogg & Hermodson, 1977; Quiocho et al., 1977; Guilliland & Quiocho, 1981). ABP has a molecular weight of 33 100 and consists of two globular domains with the sugar binding site located in a cleft between these domains. The tertiary crystal structure has been refined to 2.4 Å (Guilliland & Quiocho, 1981). ABP is active in high-affinity transport of L-arabinose (Brown & Hogg, 1972); however, it does not appear to function as a chemotaxis receptor (J. Adler, unpublished experiments). High-affinity transport of L-arabinose is inhibited by D-galactose (Brown & Hogg, 1972) which is bound by ABP with an affinity equal to that of L-arabinose binding by the molecule (Parsons & Hogg, 1974). In this study, proton nuclear magnetic resonance spectroscopy, fluorescence emission spectrophotometry, and binding thermodynamics have been used to obtain preliminary information on the solution structure of ABP and to observe the conformational changes that occur in the molecule when ligands are bound.

Experimental Procedures

The purification of ABP from *Escherichia coli* K12 was essentially as reported previously (Parsons & Hogg, 1974). *E. coli* K12 *ara A3* was grown to stationary phase in a 100-L New Brunswick Fermacel to yield 300–700 g of packed cells. The cells were broken in a French pressure cell, and ABP was purified by $(NH_4)_2SO_4$ precipitation, batchwise DEAE-cellulose filtration, DEAE-cellulose–KCl gradient column chromatography, and Sephacryl S-200 chromatography. Purification was followed by L-[^{14}C]arabinose binding assays, immuno double diffusion (using rabbit anti-ABP antisera), and electrophoresis in the absence (Davis, 1964) and presence of $NaDodSO_4$ (Laemmli, 1970).

L-Arabinose is bound to the purified ABP (Hogg & Englesberg, 1969; Quiocho et al., 1977) and can be removed by partial denaturation in 2 M guanidine hydrochloride (Miller et al., 1980). So that the efficiency of L-arabinose removal could be followed, L-[^{14}C]arabinose was added to the preparation and allowed to exchange prior to guanidine hydrochloride treatment. ABP was placed in treated dialysis tubing

† From the Department of Microbiology (A.F.C. and R.W.H.) and the Department of Pediatrics (T.A.G.), Case Western Reserve University, Cleveland, Ohio 44106. *Received June 29, 1981.* This work was supported by U.S. Public Health Service Grant AM-13791 from the National Institute of Arthritis and Metabolic Diseases.

‡ Supported by Training Grant GM-00171 of the U.S. Public Health Service. This work is from a thesis submitted to the Department of Microbiology, Case Western Reserve University, in partial fulfillment of the requirements for the Ph.D. degree. Present address: Department of Microbiology, University of Texas Health Science Center at Dallas, Dallas, TX 75235.

[1] Abbreviations: K_d, equilibrium dissociation constant; ABP, L-arabinose binding protein; ^{1}H NMR, proton nuclear magnetic resonance; DEAE, diethylaminoethyl; DTT, dithiothreitol; D_2O, deuterium oxide; ppm, parts per million; DSS, 4,4-dimethyl-4-silapentane-1-sulfonic acid, sodium salt; POPOP, 1,4-bis[2-(5-phenyloxazolyl)]benzene; PPO, 2,5-diphenyloxazole; $NaDodSO_4$, sodium dodecyl sulfate; EDTA, ethylenediaminetetraacetic acid.

0006-2960/82/0421-2227$01.25/0 © 1982 American Chemical Society

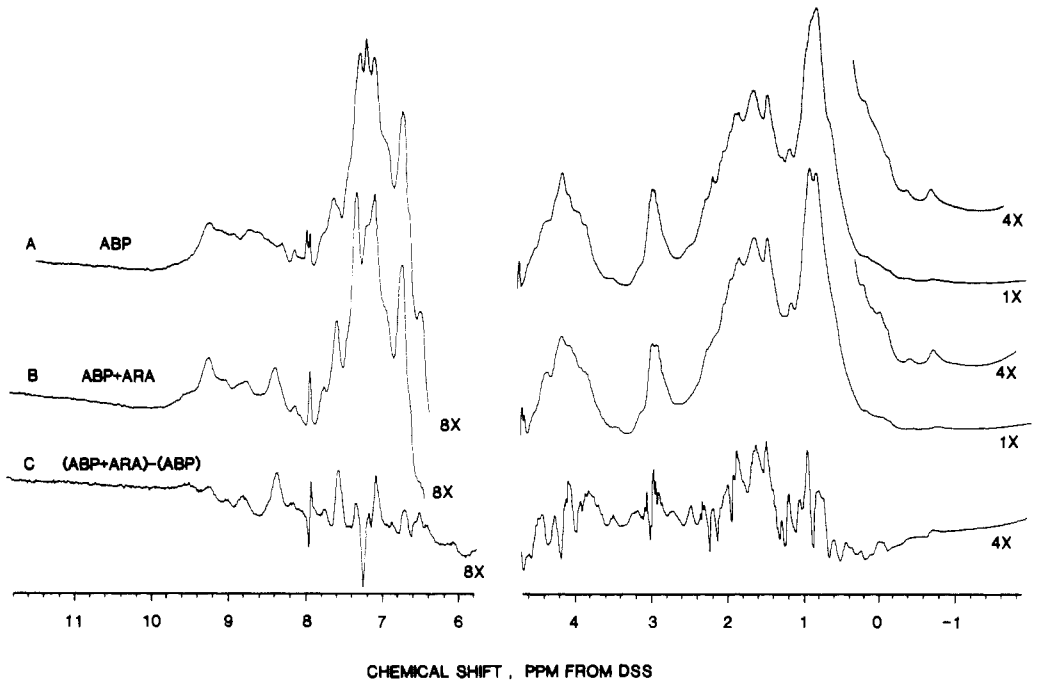

FIGURE 1: Proton NMR spectra at 270 MHz of 2 mM ABP in D_2O (50 mM potassium phosphate, pH 7.8). (A) In the absence of L-arabinose; (B) same sample as (A) with L-arabinose added in buffer (final [L-arabinose] = 4 mM); (C) a subtractive difference spectrum of (B) minus (A). The residual HDO resonance has been omitted in these spectra.

(boiled in 3 mM EDTA) and dialyzed against 500 mL of 2 M guanidine hydrochloride (Pierce) and 50 mM potassium phosphate, final pH 7.8, for 18 h at 6 °C. The protein was then passed through a Bio-Gel P-2 column (2.5 × 45 cm) eluted with 1 M guanidine hydrochloride and 50 mM potassium phosphate, pH 7.8. The protein was dialyzed extensively in 50 mM potassium phosphate and 0.1 mM DTT, pH 7.8, at 6 °C to remove all guanidine hydrochloride and finally against buffer alone.

Proton NMR studies were carried out by using a Bruker WH 270/180 pulsed Fourier-transform NMR spectrometer. Proton spectra were obtained at 270 MHz by using a 5-mm diameter probe at ambient temperature (≃20 °C). Sample volume size (0.2 mL) was optimized for H_2O or HDO suppression. Protein concentration was 1–3 mM, and sugar concentration, when added, was 4–10 mM as indicated. The ABP preparation used for the NMR studies was determined to bind approximately 0.7 mol of L-arabinose per mol of protein. Most spectra (whether in 90% H_2O or 99% D_2O) were obtained in 50 mM potassium phosphate, pH 7.8, buffer. When titrations were performed, microliter amounts of 0.2 M NaOD or DCl were added. pH values reported are uncorrected for deuterium isotope effects. Residual HDO or H_2O was suppressed by saturating the resonance for 2 s prior to the 90° (6-μs) observation pulse (Redfield & Gupta, 1971). A spectral width of 4000 Hz was used with an acquisition time of 1 s. Convolution difference spectra (Campbell et al., 1973) were obtained by subtracting a 10-Hz line-broadened spectrum from a 0.5-Hz spectrum. Final spectra were plotted at a resolution of 0.488 Hz/point. All chemical shifts are given in parts per million (ppm) from an internal DSS standard either directly or indirectly (using the HDO resonance). Spectra in 90% H_2O/10% D_2O are the result of 4000 scans, while spectra in D_2O were acquired from 2000 scans. For spectra obtained in deuterium oxide, the ABP solution was exchanged twice by dialysis for 24 h in phosphate-buffered D_2O. pK_a values were obtained by minimizing the errors between the observed data and theoretically calculated titration curves.

Equilibrium binding assays were carried out by using 10 μM ABP (in EDTA-treated dialysis tubing) in 100 mL of assay buffer (50 mM potassium phosphate and 0.1 mM DTT, pH 7.8) containing the appropriate concentration of radioactive L-[^{14}C]arabinose (60 mCi/mmol) or D-[^{14}C]galactose (60 mCi/mmol purchased from Amersham Corp.). The binding assays were allowed to reach equilibrium (18 h) while rotating at the appropriate temperature. Protein concentration was determined on samples removed from the dialysis bags by using the ABP extinction coefficient $E_{280nm} = 0.94$ (mg/mL)$^{-1}$ cm^{-1} (Newcomer et al., 1979). Samples (0.2 mL) were mixed with scintillation fluid (33% Triton X-100, in toluene, 0.067 g/L POPOP, and 2.67 g/L PPO) and counted for 10 min in a liquid scintillation spectrometer. All assays were conducted in duplicate and repeated at least once. The slopes of all plots were determined by linear regression analysis.

Fluorescence emission studies were performed on a Farred (Mark I) spectrofluorometer. Excitation and emission slits were 2.5 mm. Protein concentration was 1–10 μM, and sugar concentration was 20–50 μM. The excitation maximum was 285 nm, and fluorescence emission was scanned from 300 to 380 nm.

Results

The proton NMR spectra of native ABP in the absence and presence of its natural ligand L-arabinose are shown in spectra A and B, respectively, of Figure 1. Figure 1C is the subtractive difference spectrum of spectra A and B. It is readily apparent from the difference spectrum that ligand binding causes changes throughout the entire spectral region.

For assistance in detailing the spectral changes, the data shown in Figure 1 are presented in Figure 2A,B as convolution difference spectra which, after the removal of the broader resonances, allow the observation of single, well-resolved resonances. After simplification of the spectra in this manner, many of the changes shown in the difference spectrum in Figure 1C are still observed. The proton NMR convolution difference spectrum of ABP with D-galactose bound is presented in Figure 2C.

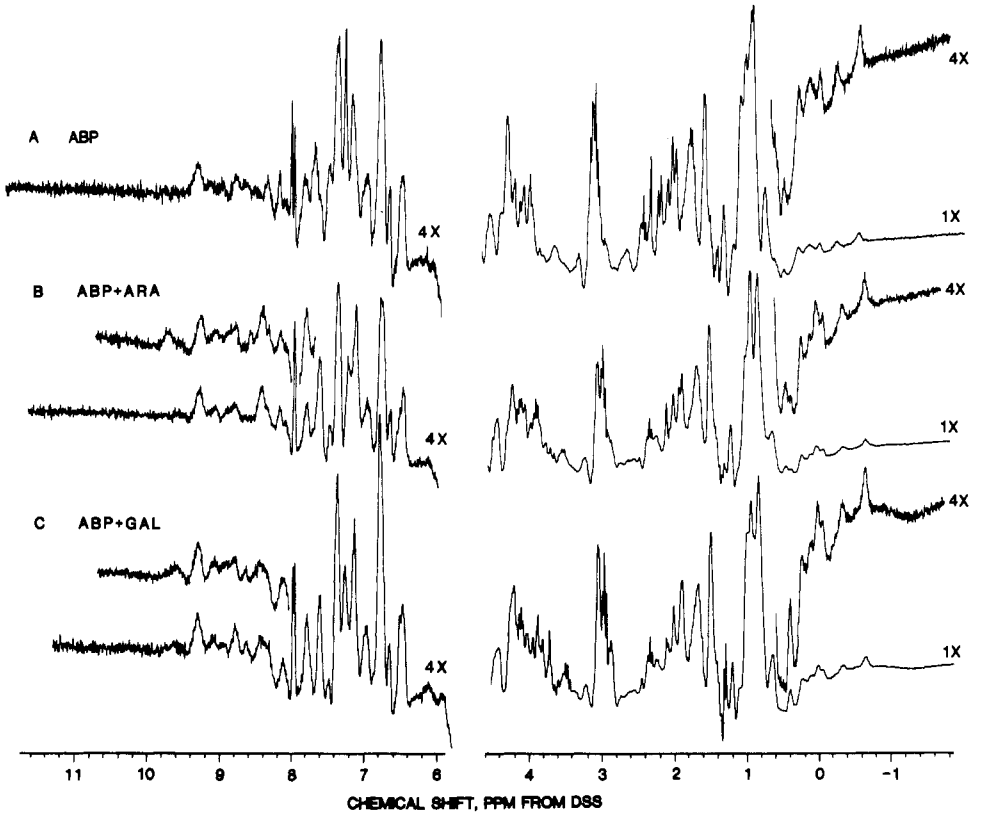

FIGURE 2: Convolution difference proton NMR spectra at 270 MHz of 2 mM ABP in D_2O (50 mM potassium phosphate, pH 7.8). (A) In the absence of L-arabinose; (B) same sample as (A) with L-arabinose added in buffer (final [L-arabinose] = 4 mM); (C) 2 mM ABP with D-galactose added in buffer (final [D-galactose] = 4 mM). Low-field insets above spectra B and C were obtained in the presence of the respective sugar (4 mM) which was added *prior* to solvent exchange with D_2O. The additional resonances therefore represent amide protons that have been protected from solvent by the binding of ligand. The sharp resonances that appear in spectra B and C between 4.0 and 3.5 ppm are due to unbound sugar. The residual HDO resonance has been omitted in these spectra.

Ligand Binding Induced Spectral Changes. A number of changes can be observed in the methyl group region (1 to −1 ppm from DSS, convolution difference spectra in Figure 2) upon binding either ligand to ABP. The most prominent change is the increase in intensity of a portion of the bulk methyl groups at 0.94 ppm. Additional changes are also observed in resonances presumed to be aromatic ring shifted methyl groups, some of which appear to shift upon binding arabinose or galactose (e.g., the shoulder at 0.53 ppm and the resonance at 0.06 ppm). The resonances near 0.0 ppm show similar alterations upon binding either ligand while the resonance near 0.5 ppm that is sensitive to ligand binding is shifted to a higher field when D-galactose is bound. These changes can be attributed to alterations in the spatial location of the methyl protons with respect to neighboring aromatic residues.

In the methylene and methine proton regions (4–1.5 ppm from DSS, Figure 2), the addition of L-arabinose or D-galactose causes many resonances to shift and/or disappear. The most prominent changes occur between 2.1 and 2.3 ppm where different changes occur upon binding either ligand, although in both cases a sharp resonance at 2.23 ppm is greatly diminished. These resonances most likely represent side-chain methylene or *S*-methyl protons of amino acid residues [i.e., Glu, Gln, Lys, Arg, or Met (Bundi & Wuthrich, 1979)] that have changed environment or have been immobilized (resonances broadened) upon the binding of ligand. The group of resonances near 3 ppm which represent the additional methylene protons of Lys, Arg, Asp, Asn, and Cys along with β protons of the aromatic amino acid residues (Bundi & Wuthrich, 1979) shows significant and similar changes after either arabinose or galactose is bound. The spectral region corresponding to the α protons of the peptide backbone, ca. 4 ppm, is also altered when either ligand is added. Caution, however, must be exercised in this region for both ligands have ring protons that appear between 4 and 3.4 ppm; thus, only the changes between 4.5 and 4 ppm can readily be attributed to the effects of binding ligand.

The majority of the resonances between 6 and 7.5 ppm originate from the CH ring protons of Phe, Tyr, and Trp residues (Bundi & Wuthrich, 1979). In this region, the most prominent alterations that occur upon ligand binding are observed for the resonances between 7.5 and 7.0 ppm. Changes are evident upon binding either arabinose or galactose with only subtle differences observed between the two ligands.

The two very sharp resonances at 8.0 ppm that coalesce when L-arabinose binds to ABP have been assigned to the C2 protons of His on the basis of their pH titration behavior (see below). The remaining broad resonances downfield of ca. 7.5 ppm are predominantly due to the slowly exchanging or nonexchangeable peptide amide protons. The spectra A and B in Figure 1 show that a large number of amide protons are unexchanged after standing in D_2O at pH 7.8. Attempts to exchange these protons at low pH (Markley, 1975a) even without heating were unsuccessful as the procedure resulted in partially denatured protein.

Upon the binding of L-arabinose or D-galactose, many changes are observed in the amide proton region; most notable is the appearance of relatively broad resonances near 8.4 ppm which differ depending on which ligand is bound. The amide protons in model peptides are generally found to appear in this 8.4-ppm region (Bundi & Wuthrich, 1979). The fact that these amide protons do not exchange with D_2O, even after several days, suggests they may be located in a region of the protein that has limited access to solvent.

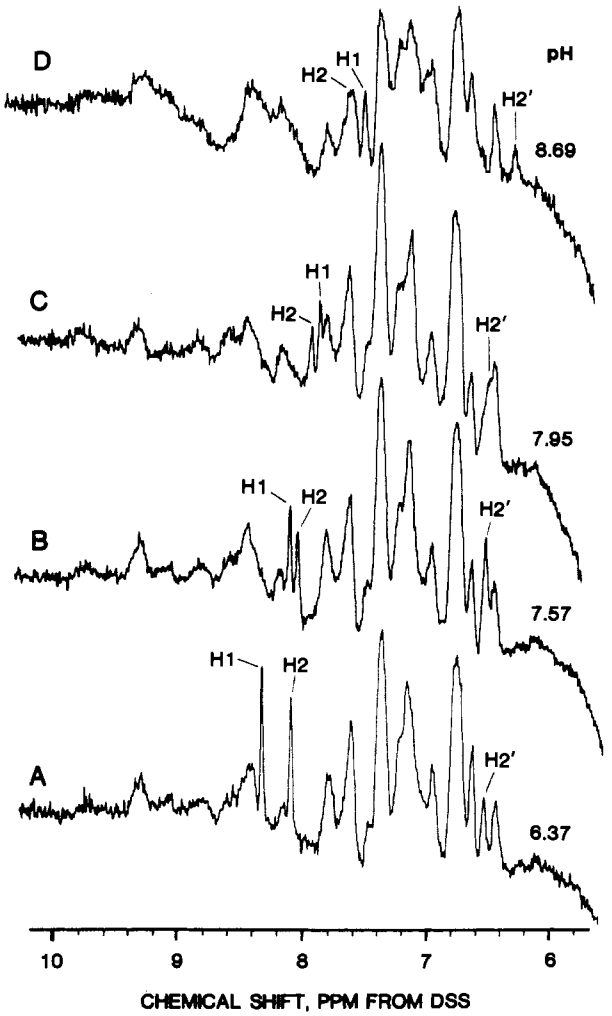

FIGURE 3: Low-field region of the proton NMR convolution difference spectra of ABP in the presence of L-arabinose at various pH values: (A) pH 6.37; (B) pH 7.57; (C) pH 7.95; (D) pH 8.69. Titratable resonances are indicated H1, H2, and H2'.

Protection of Amide Protons by Ligand Binding. For further investigation of the effects of L-arabinose and D-galactose binding on the amide proton resonances, either sugar was bound to ABP prior to exchange of the H_2O solvent with D_2O. The convolution difference spectra obtained after this treatment are identical with the spectra obtained previously for each sugar with the exception of the amide proton region (insets above spectra B and C of Figure 2) where new resonances appear which represent protons whose exchange rates have become greatly reduced upon the binding of ligand. Increased intensities are found at 9.7, 8.8, and 8.6 ppm when arabinose is used to protect exchange while increases are found at only 9.6 and 8.9 ppm when galactose is used. Spectra of the same samples obtained several days later still showed these resonances with essentially the same intensities. Convolution difference spectra obtained of ABP in 90% H_2O/10% D_2O in the absence of arabinose show many additional amide resonances including those identified above. Thus, bound L-arabinose provides significant protection from solvent, or binding elicits a conformational change in ABP which results in the protection of many amide resonances from solvent.

Characterization of Histidine Resonances. We have been able to assign the low-field resonances associated with histidine residues by obtaining spectra at various pH values as shown in Figure 3. The resonances which titrate have been labeled H1, H2, and H2', and the titration curves with and without L-arabinose are presented in Figure 4. No differences in the

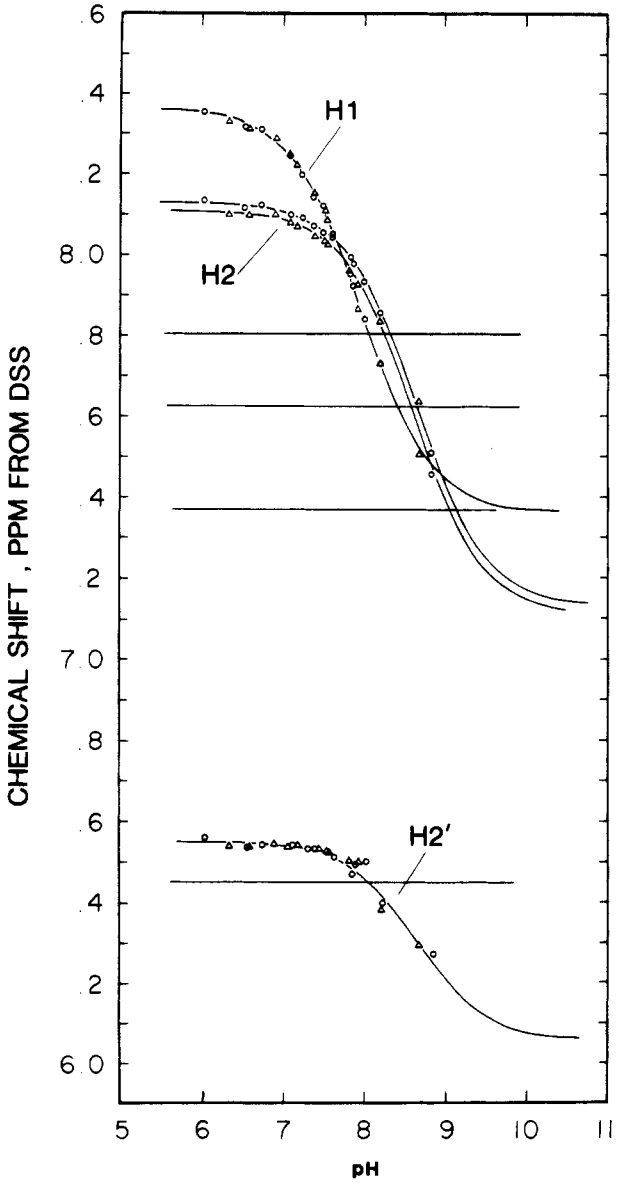

FIGURE 4: pH dependence of the titratable low-field proton resonances of ABP in the absence (○) or presence of excess L-arabinose (△). Protein concentrations were 1–3 mM ABP in 50 mM potassium phosphate in D_2O. Horizontal lines represent the chemical shifts of some of the major nontitrating resonances (see Figure 3).

titration of these resonances were observed with the addition of D-galactose compared to protein without added ligand. Resonances H1 and H2 shift in the correct direction and with a magnitude representative of C2 protons of histidine while the H2' resonance titrates as a C4 proton of histidine. For comparison, the low-pH chemical shift limits of histidine C2 and C4 protons in model peptides are approximately 8.6 and 7.3 ppm, respectively (Bundi & Wuthrich, 1979). Since we are unable to obtain the alkaline pH chemical shift limits of these resonances due to overlap, the titration curves in Figure 4 have been fit to chemical shift changes typical of histidine residues, a 1.0-ppm upfield shift for the C2 protons and a 0.5-ppm upfield shift for the C4 protons (Markley, 1975b). The calculated pK_a value for resonance H1 is approximately 8.0 and is independent of the presence or absence of arabinose. The low-pH chemical shift limit of resonance H2, however, appears dependent on the presence of absence of arabinose as shown in Figure 4 and observed in Figures 1 and 2. The calculated pK_a value for this resonance is 8.6 in either the presence or the absence of arabinose. Evidence that resonances

Table I: ABP Thermodynamic Binding Constant

	T (°C)	K_a ($\times 10^6$ M^{-1})[a]	ΔG (kcal/mol)	ΔS (eu)	ΔH (kcal/mol)[b]
L-arabinose	6.7	7.6 ± 0.9	−8.8	−2.5	
	8.0	7.0 ± 0.9	−8.8	−2.5	−9.5 ± 1.5
	16.0	5.6 ± 0.8	−8.9	−2.1	
	25.3	2.4 ± 0.4	−8.7	−2.7	
D-galactose	6.5	6.5 ± 0.8	−8.7	−10.7	
	14.7	4.4 ± 0.5	−8.7	−10.4	−11.7 ± 2.1
	24.3	1.5 ± 0.1	−8.4	−11.1	
	26.3	1.5 ± 0.1	−8.5	−10.7	

[a] Determined by Scatchard plots. The ± values represent 99% confidence limits determined from the standard deviation. [b] Determined by van't Hoff plots. Correlation coefficients of 0.96 and 0.95 were obtained for Ara and Gal, respectively. The ± values represent 99% confidence limits determined from the standard deviation.

H1 and H2 arise from protein histidine residues and not small molecule contaminants was established from the spectrum of the partially denatured protein (pH 3, 22 °C) which showed the loss of these resonances and the appearance of a new resonance (at ca. 8.6 ppm) with a chemical shift typical of histidine C2 protons. The titration of H2′ can be fit to a pK_a of 8.6 and may possibly be associated with the same histidine residue as resonance H2. pK_a values of 8.0 and higher for histidyl residues in proteins have been reported in the literature (Stoesz et al., 1979; Arata et al., 1980; Poe et al., 1979; Markley, 1975b) and may be explained in the case of ABP by the involvement of the histidine residues in ion-pair interactions with nearby acidic residues as previously identified in crystallographic studies of ABP (Guilliland & Quiocho, 1981).

Thermodynamic and Fluorescence Studies of Ligand Binding. ABP binding of L-arabinose is competitively inhibited by D-galactose. Equilibrium binding constants for both L-arabinose and D-galactose were determined at various temperatures from Scatchard plots (see Table I). The R value (moles of ligand bound per moles of ABP) varied from 0.4 to 0.7, depending on the ABP preparation utilized. Enthalpy of binding (ΔH) was calculated from a van't Hoff plot of ln K_a vs. $1/T$. Accurate binding data could not be obtained above 30 °C. Table I lists the calculated thermodynamic constants for ABP binding L-arabinose and D-galactose.

Fluorescence emission studies of ABP in the absence of ligand show an excitation maximum at 285 nm and an emission maximum at 340 nm. When L-arabinose is bound, the emission maximum is shifted to 337 nm, and the fluorescence is quenched by 10%. D-Galactose binding resulted in a similar emission shift to 337 nm; however, little or no fluorescence quenching was observed.

Discussion

Thermodynamic, fluorescence emission, and proton NMR studies were used to study L-arabinose and D-galactose binding by the periplasmic L-arabinose binding protein from *E. coli*. Both carbohydrates bind at the same site as evidenced by competitive inhibition of L-arabinose binding by D-galactose and by X-ray difference Fourier analysis of the binding region (Newcomer et al., 1979). Structurally, the 5-hydroxyl group in L-arabinose is replaced by a hydroxymethyl group in D-galactose.

ABP binds L-arabinose and D-galactose with approximately the same affinity (K_d's at 6 °C of 1.3×10^{-7} and 1.9×10^{-7} M, respectively) with only moderate differences in the enthalpy (ΔH) and entropy (ΔS) of binding observed for each sugar (Table I). As might be expected for a ligand of moderate polarity, both enthalpy and entropy contribute to the negative free energy of association. The negative enthalpy (ΔH) observed for binding either sugar is probably the result of the attractive forces formed between the sugar and the binding site residues, as well as other intramolecular interactions induced by ligand binding. A binding enthalpy of similar magnitude has been reported for the *E. coli* leucine binding protein (Berman & Boyer, 1972).

The blue spectral shift and fluorescence quenching observed when ABP binds L-arabinose are attributable to alterations in the environment of tryptophan residues (Freifelder, 1976; Guilbault, 1973; Robertson et al., 1977). ABP contains five tryptophan residues, one of which, Trp-16, is within 4 Å of the bound L-arabinose molecule (Guilliland & Quiocho, 1981). The remaining tryptophan residues are remote from the binding site. When ABP binds D-galactose, the same spectral shift is observed, but little fluorescence quenching is observed. The decrease in quantum yield observed when L-arabinose is bound is indicative of the tryptophan residue(s) responsible for the change having entered or acquired a less hydrophobic environment (Wada & Ueno, 1964; Konev, 1967; Borenboim et al., 1969). D-Galactose binding does not appear to perturb the tryptophan environments to the same extent. Blue emission shifts are often attributed to tryptophan(s) entering more hydrophobic environments, and we would therefore conclude that our observations reflect changes in a number of tryptophan residues some of which enter more hydrophilic environments while others enter more hydrophobic areas.

The proton NMR studies of the L-arabinose binding protein in the presence and absence of its substrate (L-arabinose) and its inhibitor (D-galactose) were undertaken to observe structural changes within the protein upon binding ligand. These changes may be associated with residues directly responsible for ligand binding or residues in the immediate vicinity of the binding site or as a result of more global (remote) conformational changes. Since D-galactose and L-arabinose bind to the same site and have similar binding constants and similar enthalpy and entropy changes upon binding, it is not unexpected to observe that each ligand produces similar although not identical changes in the proton NMR spectra of ABP.

Crystallographic studies show that the sugar binding site of ABP is located deep in the cleft formed between the P and Q domains of the protein (Newcomer et al., 1979). The residues contained in the binding region are Lys-10, Pro-12, Glu-14, Trp-16, Phe-17, Cys-64, Val-88, Asp-89, and Asp-90 from the P domain and Arg-151, Asn-177, Met-204, Asn-205, and Asn-232 from the Q domain (Newcomer et al., 1979). Recently, it has been determined that the side chains of Lys-10, Glu-14, Asn-205, and Asn-232, in addition to the side-chain carbonyl of Asp-90, form direct hydrogen bonds to bound arabinose (M. E. Newcomer, G. L. Guilliland, and F. A. Quiocho, unpublished experiments). On the basis of this information, several of the spectral alterations that were observed in the side-chain resonances (i.e., 1.8–2.3 and ca. 3 ppm) of the proton spectra of ABP are likely attributable to the residues involved in binding. The changes that are found in the aromatic and methyl proton regions of the spectra may also reflect alterations in the environments or a reorientation of the two aromatic residues located in the binding pocket. However, since there appears to be a number of aromatic and hydrophobic residues that are altered upon binding ligand (see Figures 1 and 2), it is possible that residues outside the binding site are sensitive to ligand binding, thus inferring the occurrence of a more extensive conformational change. Spectral

changes observed upon the addition of ligand in the amide and α-proton regions may reflect changes in the polypeptide backbone upon binding ligand, perhaps in the hinge region connecting the two domains. The increase in peak area at 8.4 ppm when either sugar is bound may indicate that a number of amide protons have had their hydrogen-bond interactions disrupted upon binding while maintaining limited exposure to solvent.

If bound prior to D_2O exchange, L-arabinose (and D-galactose to a somewhat lesser extent) will prevent the deuterium exchange of several amide protons, which suggests the protected protons are deep in the binding cleft. The differences observed between D-galactose and L-arabinose binding may reflect the accomodation within the binding site for the different ligands. However, protection could also occur in a region of the protein remote to the arabinose binding site as a result of a more extensive conformational change. Since the chemical shifts of some of these protected amide resonances are shifted from that normally observed in small peptides, it is likely that they are in a special protein environment or interaction.

Several lines of evidence have been presented that suggest the three titratable resonances, H1, H2, and H2′ (Figures 3 and 4), are due to the histidine C2 and C4 protons of two of the three histidine residues in ABP. In crystalline ABP, two histidine residues are located on the surface of the molecule removed from the binding site, while a third is in the hinge region of the binding cleft (Guilliland & Quiocho, 1981). All three histidines are shown to interact with carboxyl groups in the crystal. The cleft histidine, His-259, is least exposed to solvent and may therefore be immobilized and not readily observed. The pK_a values of the histidine residues that we observe (pK_a values of 8.0 and 8.6) are higher than normal (pK_a 6.9), presumably due to their ionic interactions with carboxyl groups. A histidine residue involved in an ion-pair interaction in another protein has been reported to have a pK_a value greater than 10 (Stoesz et al., 1979), and many others have been reported with pK_a values near pH 8 (Arata et al., 1980; Poe et al., 1979; Markley, 1975b). In our studies, one histidine resonance, H2, has been shown to be sensitive to the binding of L-arabinose. Preliminary studies on ABP isolated from a high-affinity L-arabinose transport mutant also suggest that a histidine residue may be close to a functionally important region in the protein (unpublished experiments). This mutant ABP has altered ligand binding properties, and peptide mapping analysis suggests that the mutation resides in the functionally important hinge region of the protein-containing histidine residue 198.

The studies of Quiocho and co-workers (Quiocho et al., 1980) suggest that a conformation change occurs when ABP binds L-arabinose. Using small-angle X-ray scattering, these workers observed that the radius of gyration of ABP decreased upon binding L-arabinose which they attributed to an 18° cleft closure. Our preliminary proton NMR study supports the notion that the L-arabinose binding protein undergoes a conformational change when L-arabinose is bound. The changes we observed for the most part can be attributed to alterations at or near the binding site although more extensive structural changes may not be ruled out.

On the basis of our NMR data, the binding of L-arabinose and D-galactose to ABP produces similar spectral changes that can most readily be attributed to similar structural changes occurring in and near the sugar binding site. The differences observed between the binding of these ligands may, to a large extent, reflect the different orientations of the binding site residues and polypeptide needed to accommodate these ligands. However, since none of these resonances have been unambiguously assigned to specific amino acid residues in ABP, the possibility that a larger and ligand-specific structural change occurs on binding still exists. Some data was obviously eliminated by our use of convolution difference spectra. However, it is our interpretation that the majority of the changes we observe are related to interactions in the binding site proper and represent ligand–residue accommodations. Hopefully, as we assign resonances to specific residues we will be able to establish if significant additional conformational changes occur.

References

Adler, J. (1975) *Annu. Rev. Biochem. 44*, 341–356.

Arata, Y., Honzawa, M., & Shimizu, A. (1980) *Biochemistry 19*, 5130–5135.

Berman, K., & Boyer, P. D. (1972) *Biochemistry 11*, 4650–4657.

Boos, W. (1972) *J. Biol. Chem. 247*, 5414–5424.

Boos, W. (1974) *Annu. Rev. Biochem. 43*, 123–146.

Boos, W., & Gordon, A. S. (1971) *J. Biol. Chem. 246*, 621–628.

Borenboim, G. M., Domanski, A. N., & Turoverov, K. F. (1969) *Luminescence of Biopolymers and Cells*, pp 21–26, Plenum Press, New York.

Brown, C., & Hogg, R. W. (1972) *J. Bacteriol. 111*, 606–613.

Bundi, A., & Wuthrich, K. (1979) *Biopolymers 18*, 285–297.

Campbell, I. D., Dobson, C. M., Williams, R. J. P., & Xavier, A. V. (1973) *J. Magn. Reson. 11*, 172–181.

Davis, B. J. (1964) *Ann. N.Y. Acad. Sci. 121*, 404–427.

Freifelder, D. (1976) *Physical Biochemistry*, W. H. Freeman, San Francisco.

Guilbault, G. G. (1973) *Practical Fluorescence*, pp 497–524, Marcel Dekker, New York.

Guilliland, G. L., & Quiocho, F. A. (1981) *J. Mol. Biol. 146*, 341–362.

Hogg, R. W., & Englesberg, E. (1969) *J. Bacteriol. 100*, 423–432.

Hogg, R. W., & Hermodson, M. A. (1977) *J. Biol. Chem. 252*, 5135–5141.

Knoev, S. V. (1967) *Fluorescence and Phosphorescence of Proteins and Nucleic Acids*, p 81, Plenum Press, New York.

Koshland, D. E. (1977) *Science (Washington, D.C.) 196*, 1055–1063.

Kreishman, G. P., Robertson, D. E., & Ho, C. (1973) *Biochem. Biophys. Res. Commun. 53*, 18–23.

Laemmli, U. K. (1970) *Nature (London) 227*, 680–685.

Langridge, R., Shinagawa, H., & Pardee, A. B. (1970) *Science (Washington, D.C.) 169*, 59–61.

Manuck, B. A., & Ho, C. (1979) *Biochemistry 18*, 566–573.

Markley, J. L. (1975a) *Biochemistry 14*, 3546–3554.

Markley, J. L. (1975b) *Acc. Chem. Res. 8*, 70–80.

McGowan, B. B., Silhavy, T. J., & Boos, W. (1974) *Biochemistry 13*, 993–999.

Miller, D. M., Olsen, J. S., & Quiocho, F. A. (1980) *J. Biol. Chem. 255*, 2465–2471.

Neu, H. C., & Heppel, L. A. (1965) *J. Biol. Chem. 240*, 3685–3692.

Newcomer, M. E., Miller, D. M., & Quiocho, F. A. (1979) *J. Biol. Chem. 254*, 7529–7533.

Parsons, R. G., & Hogg, R. W. (1974) *J. Biol. Chem. 249*, 3602–3607.

Poe, M., Hoogsteen, K., & Matthews, D. (1979) *J. Biol. Chem. 2545*, 8143–8152.

Quiocho, F. A., Guilliland, G. L., & Phillips, G. N. (1977) *J. Biol. Chem. 252*, 5142–5149.

Quiocho, F. A., Miller, D. M., Newcomer, M. E., Guilliland, G. L., Pflugrath, J. W., & Charletta, D. A. (1980) *J. Supramol. Struct., Suppl. 4*, 76.
Redfield, A. G., & Gupta, R. K. (1971) *J. Chem. Phys. 54*, 1418–1419.
Robertson, D. E., Kroon, P. A., & Ho, C. (1977) *Biochemistry 16*, 1443–1451.
Stoesz, J. D., Malinowski, D. P., Redfield, A. G. (1979) *Biochemistry 18*, 4669–4675.
Szmeleman, S., Schwartz, M., Silhavy, T. J., & Boos, W. (1976) *Eur. J. Biochem. 65*, 13–19.
Wada, A., & Ueno, Y. (1964) *Biopolym. Symp. 1*, 343–364.
Weiner, J. H., & Heppel, L. A. (1971) *J. Biol. Chem. 246*, 6933–6941.

Interaction of Oleoyl Coenzyme A with Phospholipid Bilayers†

Alice H. Lichtenstein, Donald M. Small, and Peter Brecher*

ABSTRACT: The effect of oleoyl coenzyme A (CoA) on three phospholipid bilayer systems, human red blood cell ghosts, egg yolk lecithin dispersions, and unilamellar lecithin vesicles, was studied. Addition of oleoyl-CoA to sealed, right-side-out, human red blood cell ghosts resulted in a loss of latent NADH–cytochrome *c* oxidoreductase activity. The turbidity of lecithin dispersions decreased as a result of the addition of oleoyl-CoA in a concentration-dependent manner. This decrease in turbidity was influenced by the mode of addition of oleoyl-CoA to the phospholipid, and the most pronounced decrease was observed when oleoyl-CoA was dried together with the lecithin prior to resuspension in an aqueous solution. The presence of cholesterol (lecithin:cholesterol molar ratio 2:1) diminished the effect of oleoyl-CoA on the turbidity of the lecithin dispersions. Addition of oleoyl-CoA to unilamellar vesicles, which contained 5,6-carboxyfluorescein, increased the leakage of the dye from the vesicles in a concentration-dependent manner. This effect was diminished when cholesterol was incorporated into the vesicles (lecithin:cholesterol molar ratio 2:1). The interaction of oleoyl-CoA with lecithin was further studied by preparing mixtures where the lipids were dried together prior to sonication and had lecithin:oleoyl-CoA molar ratios of either 100:1 or 10:1. The resulting complexes were characterized by gel filtration and sucrose density gradient ultracentrifugation. Oleoyl-CoA was associated with particles having a size indistinguishable from that of unilamellar vesicles. At the higher oleoyl-CoA concentration, the complex formed was readily detected by density gradient ultracentrifugation because of the increased particle density. Addition of albumin to the mixtures caused dissociation of oleoyl-CoA from the vesicles but did not result in vesicle disruption under the conditions employed. The results show that oleoyl-CoA forms stable complexes with phospholipid bilayers and suggest that such complexes modify the permeability of the bilayer system.

Long-chain acyl-CoA[1] molecules have been proposed to have a regulatory role in intracellular metabolism. Support for such an effect is based primarily on the in vitro effect of either palmitoyl- or oleoyl-CoA on the activity of several enzymes localized in the cytosol (Kawaguchi & Bloch, 1976; Edgar & Bell, 1979). The physiological significance of such regulation is controversial since long-chain acyl-CoA forms micelles at concentrations close to that required for the inhibition of enzyme activity (Zahler et al., 1968), suggesting that the inhibition observed in vitro may be due to nonselective detergent effects. Recent studies have shown inhibition of several enzymes by palmitoyl-CoA at concentrations below its putative critical micellar concentration (Edgar & Bell, 1979) and where the effect of the CoA derivative was distinguished from that of other detergents (Wititsuwannakul & Kim, 1977; Hsu & Powell, 1975; Kawaguchi & Bloch, 1974), suggesting that acyl-CoA may have a regulatory role in vivo.

An understanding of what actually occurs in vivo is complicated by observations showing that intracellular proteins exist that bind long-chain acyl-CoA (Mishkin & Turcotte, 1974; Jamdar, 1979) and may prevent micelle formation. Further, a recent report indicated that the critical micellar concentration of palmitoyl-CoA was above 30 μM and the aggregation number was between 20 and 40 (Powell et al., 1981). These values are different than the previously reported values of 3–4 μM and 1000 (Zahler et al., 1968). Finally, there is no direct evidence on the state of long-chain acyl-CoA monomers, or micelles, bound to proteins or membranes within the cell. Most previous studies on acyl-CoA–enzyme interactions were performed with soluble enzymes often found in the cytosol. It is now known that many of the enzymes that utilize long-chain acyl-CoA as substrates are membrane bound and are localized on the outer (cytoplasmic) side of sealed microsomal vesicles (Bell et al., 1981). Therefore, acyl-CoA must interact with the membrane prior to or during its metabolism. Previous studies showed an association between palmitoyl-CoA and liver microsomes (Lamb & Fallon, 1972). Recent studies by Polokoff & Bell (1978) suggested that at physiological concentrations, palmitoyl-CoA can penetrate rat liver microsomes to become accessible to an ethanol acyltransferase, shown to be located on the inner (lumenal) side of the microsomes. That study and those of Jamdar (1979) and Lichtenstein & Brecher (1980) have shown that acyl-CoA can alter the permeability of rat liver microsomes as reflected by loss of latent mannose-6-phosphatase activity.

The precise nature of the interaction between long-chain acyl-CoA and biological membranes is not understood. This study describes the interaction of oleoyl-CoA with human red

† From the Department of Medicine and Biochemistry, Boston University School of Medicine, Boston, Massachusetts 02118. *Received April 7, 1981.* This work was supported by U.S. Public Health Service Grants HL 12869 and HL 26335 and the U. A. Whitaker Fund.

[1] Abbreviations: 5,6-CF, 5,6-carboxyfluorescein; CoA, coenzyme A; NADH, reduced nicotinamide adenine dinucleotide; Tris, tris(hydroxymethyl)aminomethane; Hepes, *N*-(2-hydroxyethyl)piperazine-*N*′-2-ethanesulfonic acid.

0006-2960/82/0421-2233$01.25/0 © 1982 American Chemical Society